

Synthesis of diamond microcrystals with a unique diversity of NiN_x color centers by spontaneous crystallization using a nickel catalyst and europium oxide

Vladimir Yu. Osipov, Fedor M. Shakhov, Andrei D. Trofimuk and Kazuyuki Takai

Contents

S1. Synthesis of diamond microcrystals.....	S1
S2. Characterization: Electron paramagnetic resonance.....	S3
S3. Photoluminescence spectra of microcrystals of Group 6 synthesized with the addition of europium(III) oxide.....	S4

S1. Synthesis of diamond microcrystals

Microcrystalline diamonds (sample D1) were synthesized under high pressure (5 GPa) and temperature (1650 °C) in quasi-equilibrium conditions using a nickel catalyst according to the previously described procedure.^{S1} The synthesis time of diamond crystallites was 90 s. The scheme of the high-pressure cell used for the synthesis of diamond microcrystals can be found in Ref. S2. It should be noted that in order to implement the conditions of the so-called *spontaneous crystallization* and high nitrogen content in the crystals, nitrogen getter and micron-sized diamond seeds, *i.e.* crystallization centers, were not added to the charge. The main operations used in this synthesis are as follows. The mixture was prepared from powdered electrode graphite (grade EG15, ash content <0.05 wt%, particle size 315–400 µm) and a commercial nickel powder (grade PNE-1, particle size up to 71 µm), taken in a 50:50 (w/w) ratio. Graphite and nickel powders were supplied by manufacturers from Russia. At a pressure of 5 GPa, nickel melts at ~1630 °C and gradually dissolves graphite in itself. The dissolved carbon is gradually released from the molten nickel in the form of diamond crystallites up to ~160 µm in size. The above temperature and pressure correspond to the conditions for diamond nucleation and growth of diamond crystals from carbon dissolved in nickel. Due to the mass transfer of the carbon material through the molten nickel, the synthesized microcrystals are enriched in nickel. After completion of the synthesis, diamond microcrystals, which we called D1, were isolated from the sinter by etching the metallic nickel and non-diamond phase in hot acids. The resulting diamond powder was then fractionated using a 100 µm sieve. Other important details and features of the growth of such microcrystals at high pressure and high temperature can be found in Refs. S1 and S3.

Microcrystals of the second type (D1-bis) were obtained by adding about ~5 wt% europium(III) oxide powder (particle size up to 100 µm) to the pre-prepared graphite–nickel (50 : 50, w/w) charge to obtain a C–Ni–Eu₂O₃ mixture of the composition 47.6 : 47.6 : 4.8. Europium oxide powder was supplied by a manufacturer from Russia. The yield of the diamond phase from graphite was about 31 and 23%, respectively, for the synthesized microcrystalline samples D1 and D1-bis. Both samples contain nickel and nitrogen, and the content of impurity nitrogen in the carbon-substituting positions is approximately the same in the D1 and D1-bis microcrystals. In addition to nickel and nitrogen, the microcrystals contain a certain amount of various nickel–nitrogen (Ni–N) complexes, which are detected by optical luminescence. In both cases, the synthesized crystals before fractionation had a size of 30 to 160 µm. The electron microscopy images of the obtained crystallites are shown in Figure S1. They were obtained using a JEOL JSM-6390 scanning electron microscope (Japan). It can be seen that the microcrystals of both types have an arbitrary unfaceted shape with a coarse roughness, and only a small

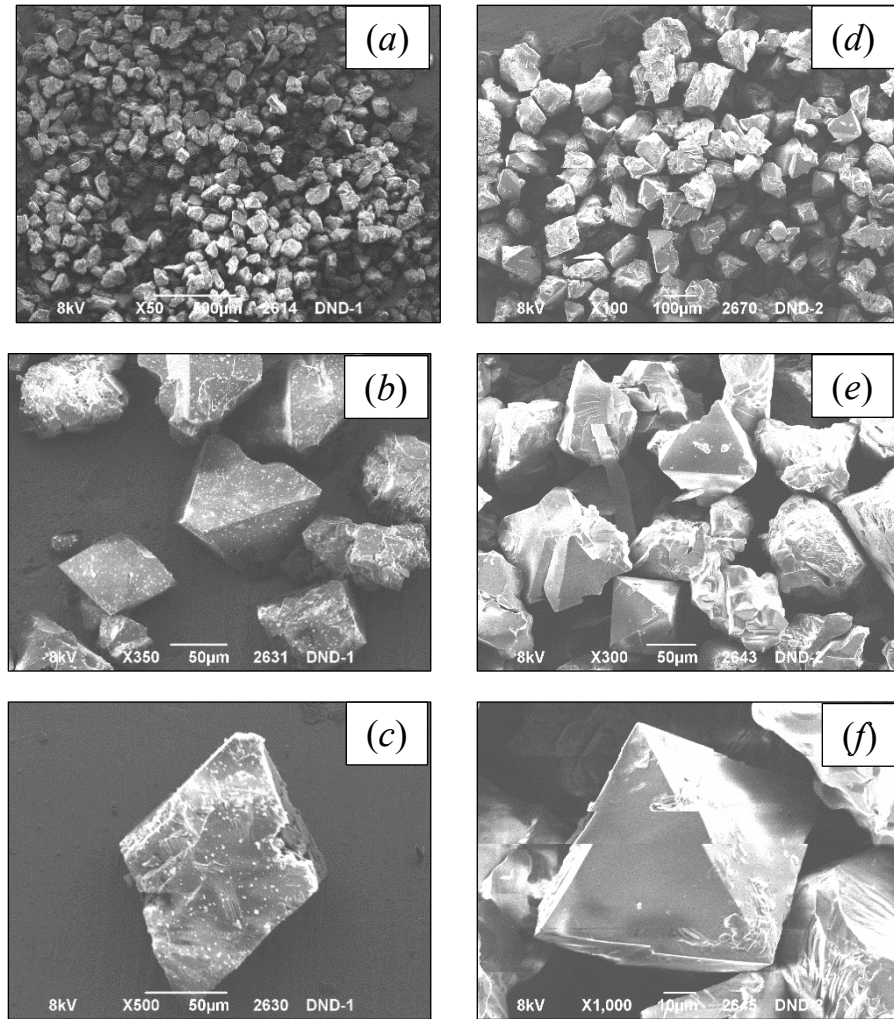


Figure S1 Scanning electron microscopy images of (a)–(c) D1 microcrystals and (d)–(f) D1-bis microcrystals obtained at magnifications of (a) $\times 50$, (b) $\times 350$, (c) $\times 500$, (d) $\times 100$, (e) $\times 300$ and (f) $\times 1000$ and an electron beam accelerating voltage of 8 kV. Scale bars, μm : (a) 500, (b),(c),(e) 50, (d) 100 and (f) 10. Some perfect or incompletely grown microcrystals of octahedral shape are clearly visible in panels (b), (e) and (f).

part of the crystallites exhibits full or partial faceting [Figure S1(b),(f)]. Despite the unfaceted arbitrary shape of most D1 and D1-bis microcrystals [Figure S1(b),(e)], they have a fairly high quality of the crystal lattice in combination with a relatively high (~ 380 – 410 ppm) concentration of substitutional nitrogen impurities. This is evidenced by electron paramagnetic resonance (EPR) studies of microdiamonds. Surprisingly, D1-bis microdiamonds obtained using europium(III) oxide have a higher content of impurity nickel (Ni_s^-) in carbon-substituting positions. At the same time, in the grown D1-bis diamonds after their extraction from the batch after synthesis, the europium oxide phase is not detected by X-ray diffraction analysis. Elemental analysis carried out by X-ray fluorescence spectroscopy shows that the europium content in D1-bis diamonds is about ~ 7 ppm (Table S1). Using this method of elemental analysis, copper was unexpectedly detected in samples D1 and D1-bis at a level of 140–280 ppm. It gets there as a parasitic undesirable impurity during the synthesis process from high-pressure cell materials.

The total nickel content in both samples, according to the data presented in Table S1, significantly exceeds that of Ni_s^- ions determined by the EPR method. This is due to the fact that the main amount of nickel is in the diamond matrix in an aggregated form, *i.e.* in the form of nanoparticles ranging in size from 7 to 15 nm, which is confirmed by the X-ray diffraction method.^{S4}

Table S1 Metal content according to X-ray fluorescence spectroscopy.

Sample	Nanosized inclusions	Element content (ppm)			
		Ni	Cu	Zr	Eu
D1	Nickel (size <15 nm)	1033	283	1.8	–
D1-bis	Nickel (size <15 nm)	524	139	–	6.7

S2. Characterization

Electron paramagnetic resonance

The EPR study of the samples was carried out at the Research Center for Micro-Nano Technology of Hosei University (Koganei, Tokyo, Japan). The spectra were recorded at low temperature ($T = 90$ K) using a JEOL JES-FA 300 EPR spectrometer (Japan) at a microwave frequency of 9.070 GHz. The microwave power used to record the EPR spectra was 3 μ W. Diamond powder (about 20–22 mg) was poured into a narrow quartz capillary (outer diameter 2.1 mm, height 45 mm), which was placed at the bottom of a standard long quartz EPR tube. The details of the EPR measurements were disclosed in our previous work.⁵⁵ The magnetic field was measured using a standard Hall sensor glued to one of the poles of the electromagnet. Note that in all presented EPR spectra, the uncorrected value of the magnetic field obtained from the Hall sensor is plotted along the horizontal axis, and for precision calculations, the field was corrected by several Gauss downwards using a powder EPR standard with a g-factor of 2.0024.

The EPR spectra of the D1 and D1-bis samples obtained at 90 K showed the presence of isolated nickel and nitrogen impurities in the diamond lattice in the substitutional form. All lines in the EPR spectra of samples D1 and D1-bis are equally broadened due to the high concentration of both paramagnetic nitrogen (the main broadening agent in the system) and other *spin-half* paramagnetic species with the same g-factor. This implies the dipole–dipole mechanism for line broadening from paramagnetic spins. Figure S2(a),(b) shows the separation of the integrated EPR spectra of samples D1 and D1-bis into the contours from the substitutional nitrogen, nickel Ni_s^- and another unrecognized defect. It is known that the signal from the substitution nitrogen has a triplet hyperfine structure associated with the magnetic moment of the ^{14}N nucleus, and the signal from the Ni_s^- centers ($g = 2.0319$) has a singlet Lorentzian contour. Thus, each of the spectra is decomposed into five individual Lorentzian contours. In this case, a fifth Lorentzian contour of the prevailing width is constructed on each spectrum for its optimal fitting with a minimum number of Lorentzian contours. It should be emphasized that the nitrogen signal consists of three equally spaced Lorentzian lines (centered at ~ 320.56 , ~ 323.7 and ~ 326.9 mT) with approximately the same intensity and width in all three components [see Figure S2(a),(b), blue line]. All lines of this triplet are equally strongly self-broadened due to the high concentration of the prevalent paramagnetic impurities (mainly nitrogen). The remaining two EPR signals in approximately the same range are due to substitutional nickel impurities and some other paramagnetic defects, which cause a broad EPR line (at ~ 323.7 mT) under the central nitrogen triplet signal ($g = 2.0024$). For both EPR spectra, we can see an intense broad signal near the central line ($g = 2.0024$) [see Figure S2(a),(b), orange contours]. This broad signal, originating from the third paramagnetic agent, can be associated with non-nitrogen centers, such as negatively charged vacancies with spin $S = 3/2$, or compact paramagnetic clusters based on several neighboring nitrogen atoms. The exact attribution of the additional central signal [Figure 2(a),(b), orange contours] is difficult due to many alternatives and is beyond the scope of this article. The signals from nickel are shown in Figure S2(a),(b) as low-intensity contours (red line) of

the Lorentzian shape (centered at 319.1 mT), overlapping with low-field satellites of the signals from nitrogen (P1). The integrated intensity of this signal at ~319.1 mT was used to determine the concentration of nickel ions Ni_s^- in the diamond matrix using the described method.⁵⁵

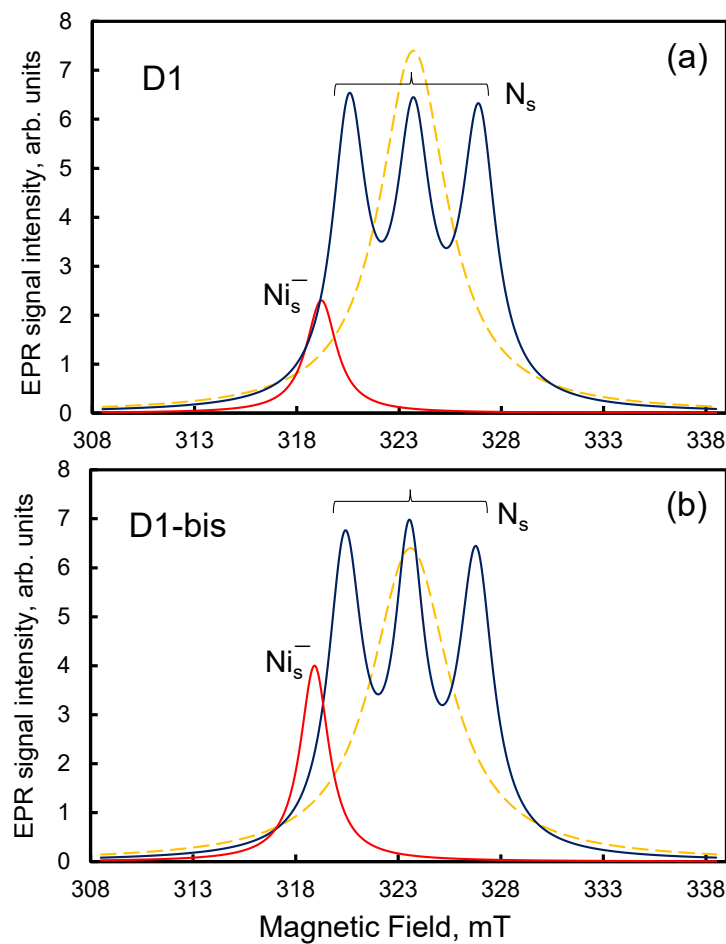


Figure S2 Integrated EPR spectra of (a) sample D1 and (b) sample D1-bis after decomposition into five components: three components of the nitrogen triplet signal (blue contour) and two singlet signals, one from substitutional nickel impurities (red contour) and the other (orange contour) from intrinsic spins $\frac{1}{2}$ in the diamond lattice. The broad Lorentzian contour (orange dashed line) originates from poorly identifiable paramagnetic defects, probably associated with nitrogen-based impurity clusters. The spectra were recorded at a microwave frequency of 9.071 GHz and $T = 90$ K.

S3. Photoluminescence spectra of microcrystals of Group 6 synthesized with the addition of europium(III) oxide

Luminescence spectra were studied using the NTEGER-Spectra II setup (NT-MDT Spectrum Instruments, Russia) with the exciting radiation focused using a $100\times$ micro objective at wavelengths of 532 and 633 nm. The exciting laser radiation was focused directly onto the surface of the diamond microcrystal selected for analysis or into the volume of the diamond crystallite at some distance from the surface. Luminescence studies for each microcrystalline sample (D1 or D1-bis) were carried out by recording the spectra on 40–50 selected microcrystals and their subsequent analysis with division into groups with characteristic spectral signatures.

In the ensemble of D1-bis microcrystals, it is easy to distinguish up to six groups of different particles with different luminescence spectra. One of these groups of particles (Group 6) has the luminescence spectrum shown in Figure S3 (red line). This spectrum consists of a broad (600–770 nm) emission

spectrum of NV^- centers and characteristic luminescence bands of Eu^{3+} centers enclosed in the diamond matrix both as isolated impurities and, perhaps, as oxide forms. This is due to the fact that a number of fine features visible in the luminescence spectrum of particles in Group 6 (red line) coincide well with the position of the characteristic spectral lines of europium(III) oxide used to synthesize D1-bis microcrystals (Figure S3). Among these features, the most intense is the doublet of emission spectral lines at 615.5 and 621.2 nm. In both luminescence spectra, the following intracenter emission optical transitions associated with Eu^{3+} are visible: $^5\text{D}_0 \rightarrow ^7\text{F}_0$, $^5\text{D}_0 \rightarrow ^7\text{F}_1$, $^5\text{D}_0 \rightarrow ^7\text{F}_2$ and $^5\text{D}_0 \rightarrow ^7\text{F}_4$.

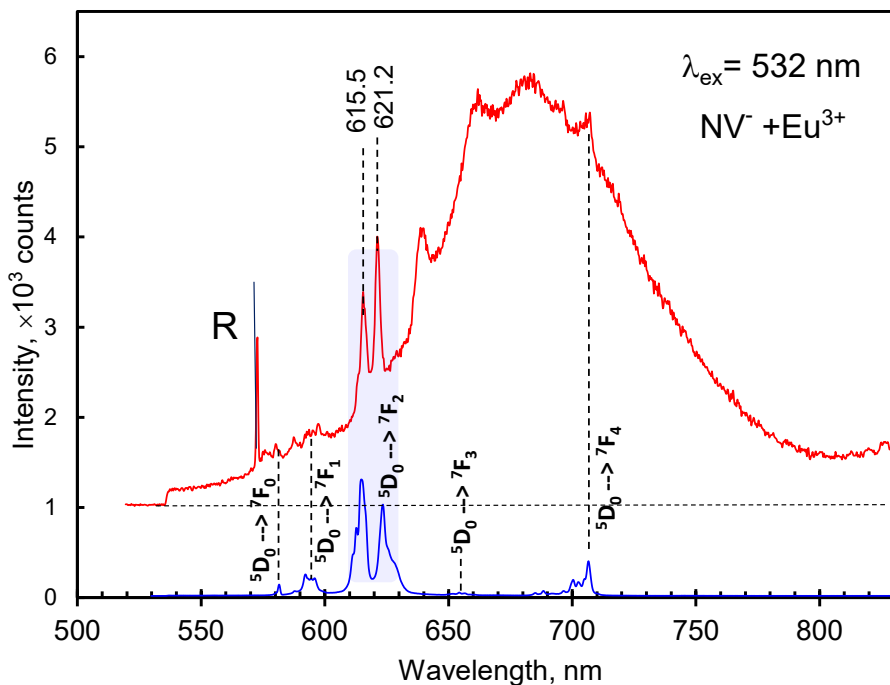


Figure S3 Photoluminescence spectrum of Group 6 microdiamond particles with NV^- centers and europium-containing inclusions (red line) compared with the emission spectrum of pure europium(III) oxide (blue line). The figure shows the identifiable intracenter $4f\ ^5\text{D}_0 \rightarrow ^7\text{F}_J$ ($J = 0-4$) optical transitions in the Eu^{3+} ion. To facilitate comparison of fine features in both spectra, the emission spectrum of D1-bis particles is shifted vertically by one scale division. The Raman line of diamond is designated by the letter R. The excitation wavelength is 532 nm.

References

- S1 F. M. Shakhov, V. Yu. Osipov, A. A. Krasilin, K. Iizuka and R. Oshima, *J. Solid State Chem.*, 2022, **307**, 122804.
- S2 F. M. Shakhov, A. M. Abyzov and K. Takai, *J. Solid State Chem.*, 2017, **256**, 72.
- S3 I. E. Kaliya, V. Y. Osipov, F. M. Shakhov, K. Takai, K. V. Bogdanov and A. V. Baranov, *Carbon*, 2024, **219**, 118839.
- S4 F. M. Shakhov, R. Oshima and V. V. Popov, *J. Phys. Chem. Solids*, 2024, **185**, 111770.
- S5 V. Yu. Osipov, F. M. Shakhov, N. M. Romanov and K. Takai, *Mendeleev Commun.*, 2022, **32**, 645.